SUPPORTING INFORMATION FOR

Confined Water Molecules in Binary Mixtures of Water and 2,6-Lutidine Near Lower Solution Critical Temperature

Alexander A. Korotkevich* and Huib J. Bakker

AMOLF, Science Park 104, 1098 XG Amsterdam, The Netherlands

Table of contents

Linear infrared spectra treatment scheme....1

Linear infrared spectra of systems with X > 0.5 1

Fitting routine description 2

Description of the local hot state associated anisotropy....3

Divergence of the excited state anisotropy upon subtraction of an isotropic local hot state response 3

Selected data with fit results obtained with the model described in the text....4

Temperature dependence of the vibrational relaxation rate 7

Temperature dependence of the fraction and reorientation dynamics of the slow water fraction...7

Raw anisotropy dynamics....8

Linear infrared spectra treatment scheme

In order to accurately extract the shape of OD-stretch absorption band we performed two series of measurements. The first series consisted of measurements of mixtures of 2,6 lutidine and isotopically diluted water and the second series consisted of solutions with the same lutidine content and normal water (no isotopical dilution). The spectra obtained in the second series were subtracted from spectra from those in the first series. Since the only difference of these two series is the presence of HDO molecules, this procedure yields the spectrum of the OD-stretch vibration.

Linear infrared spectra of systems with X > 0.5

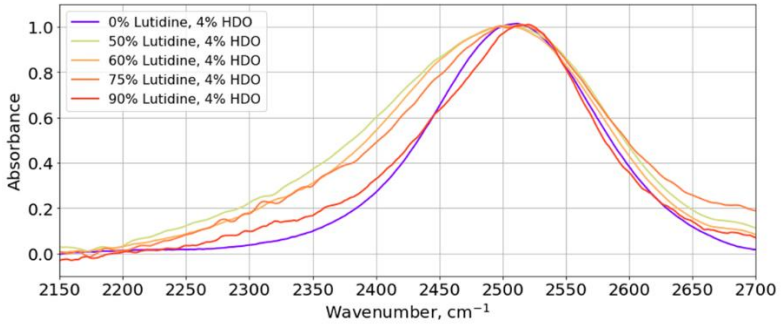

Figure S1. Linear absorption spectra in the frequency region of the OD stretch vibration.

As can be clearly seen, the absorption peak narrow when the lutidine content increases above X = 0.5, reaching a shape quite close to the shape of neat isotopically diluted water at X = 0.9.

Fitting routine description

We have performed the fitting of the time resolved data according to the kinetic scheme described in the main text. This approach is closely related to the one described by Lotze et al.[1] Here we provide the details of the method necessary to program the procedure in Python 3.7 and we explain how the procedure was modified to fit the data, compared to the previously described approach.

Given a rate matrix (D) corresponding to the kinetic scheme described in the main text, and an initial guess for the rate constants and time-zero populations, a population matrix is computed as a solution of the system of ordinary differential equations (rate equations):

$$N = \exp(Dt)N(0) \tag{S1}$$

where N is a m×3 population matrix, where m is the number of delay times probed, D is a 3×3 rate matrix, the t values are the probed delay times, N(0) is a vector containing the initial populations of each of the 3 states. Each column of N is filled with the populations of each state at each delay time. The product on the right-hand side of the equation is a matrix product. The computation is performed using **numpy.mat()** to perform the matrix multiplication and **scipy.linalg.expm()** for matrix exponential. Initial populations are normalized to make the sum of populations equal to 1 at each delay time. The time zero populations of the two excited states are 0.5, and the time-zero population of the local hot state is 0. The evolution is determined by the kinetic scheme and the initial guess of the rate constants.

After this computation a system of linear equations determining the spectral shapes was solved:

$$N\sigma = \Delta\alpha_{iso} \tag{S2}$$

to determine a σ - 3×32 spectral shapes matrix . Each row of the matrix contains a normalized transient absorption value corresponding to each of the frequencies probed. This was achieved by using the linear least square algorithm **numpy.linalg.lstsq()**. $\Delta\alpha_{iso}$ is to be perceived as the m×32 array calculated directly from experimental data.

Given the spectral shapes and the population matrix, a χ^2 was constructed analogously to Lotze et al. in order to perform a fit to find the optimal rate constants for its minimization. This minimization is performed using a nonlinear least squares algorithm using **scipy.optimize.minimize()** function. The found rate constants are used again at the start of the following optimization step. This cycle is repeated before the unit convergence of the χ^2 value is reached, resulting in optimal rate constants and spectral shapes.

We fitted $\Delta\alpha_{\parallel}$ and $\Delta\alpha_{\perp}$ in order to extract state-associated anisotropies. To this purpose, an anisotropy (*R*) matrix with the same dimensions as the population matrix was implemented. Each column of the matrix contains the state-associated anisotropy value at the particular delay time. Using an initial guess, the values of anisotropies were calculated according to equations 5 and 6 of the main text. Given a guess for *R*, the spectral shapes matrix and the population matrix from the fit of the isotropic data, a first approximations of $\Delta\alpha_{\parallel}$ and $\Delta\alpha_{\perp}$ are computed. While *RN* was an elementwise product, the result of the product was used to perform a matrix multiplication with σ. Using this approximation again a corresponding χ^2 was constructed analogously to Lotze et al.

Differently from this approach, we also normalized the χ^2 value at the magnitude of the response in order to improve the description at longer delay times. To fit $\Delta\alpha_{\parallel}$ and $\Delta\alpha_{\perp}$ the sum of the χ^2s for $\Delta\alpha_{\parallel}$ and $\Delta\alpha_{\perp}$ was minimized. Minimization of the χ^2 yields a set of parameters describing the anisotropy which are then used to recalculate $\Delta\alpha_{\parallel}$ and $\Delta\alpha_{\perp}$. Repeating the steps until convergence is reached yields the optimal state-associated anisotropy parameters.

Description of the local hot state associated anisotropy

An approach to describe the local hot state anisotropy is based on the idea that the state created after the vibrational relaxation partly inherits the anisotropic distribution of the excited OD-groups, similar to the procedure described by Rezus et al[2]. A general expression describing this anisotropy is:

$$R_h(t) = \frac{a \times \int_0^t \sum dN_{e,i}(\tau) R_{e,i}(\tau) f(\tau)}{\int_0^t \sum dN_{e,i}(\tau)} \qquad \text{(S3)}$$

Here R_h is the anisotropy of the local hot state, a is the fraction of the inherited anisotropy, $R_{e,i}$ is the anisotropy of the *ith* excited state, $dN_{e,i}(\tau)$ is the decrement of the population of the *ith* excited state during the period $d\tau$ obtained from the vibrational relaxation kinetic model, and $f(\tau)$ reflects the anisotropy decay of the local hot state.

We find that the expression could be simplified in the following way:

1) Based on eq. 5 anisotropy of the excited state is bimodal and we assumed that only slow water molecules contribute to the anisotropy of local hot state. For that reason we excluded a time dependent term from the expression for $R_{e,i}$
2) Based on the signal to noise ratio at long delay time we find that including a decay of the anisotropy of the local hot state adds an additional parameter to the model without adding an improvement into the fitting quality. For that reason, we consider anisotropy of the local hot state to be non-relaxing ($f(\tau) = 1$)
3) Based on (1) and (2) the integral in S3 contains only time dependent terms of the summation of $dN_{e,i}$ and the integral is divided out by the value $\int_0^t \sum dN_{e,i}(\tau)$. Since the identical set of parameters is used for each $R_{e,i}$ equation S3 simplifies to $R_h = a \times R_{slow}$.

Divergence of the excited state anisotropy upon subtraction of an isotropic local hot state response

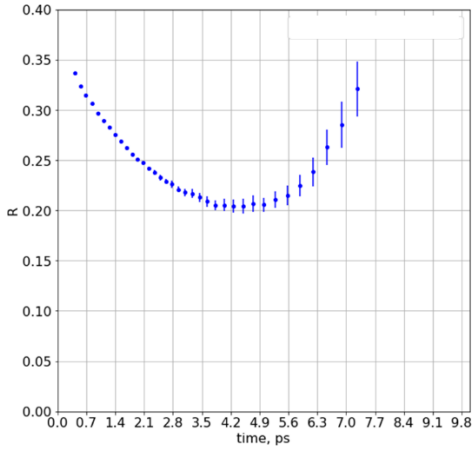

Figure S2 Anisotropy dynamics of an X = 0.15 mixture, constructed by subtracting an isotropic local hot state response from the $\Delta\alpha_{\parallel}$ and $\Delta\alpha_{\perp}$ data.

Selected data with fit results obtained with the model described in the text

We show in the selected spectra and the extracted spectral signatures. There are three main sources of changes regarding the concentration dependence of the spectra:

1) a change in relative intensity of the excited state spectrum and the local hot state spectrum comes from the fact that with the increased solute fraction the relative amount of water within the excited volume decreases leading to both smaller cross-section and eventually to the final lower local temperature. It is well known that the heating difference spectrum has higher intensity at higher temperatures
2) a change in the relaxation rate – is discussed in the text
3) a change in the linewidth (for both ground state bleaching/stimulated emission and the induced absorption) – comes from the fact that the strong hydrogen bonds are formed between the solute and water that leads to the broadening of the absorption band (same as in conventional FTIR). That leads to the shift of the point where the spectrum crosses 0.

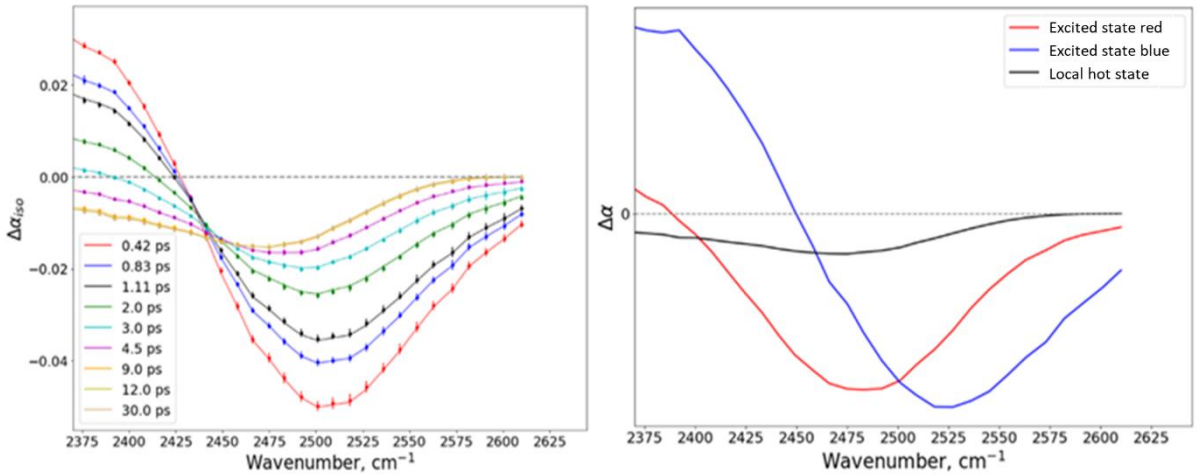

Figure S3. Transient spectra and spectral components of an X = 0.02 mixture

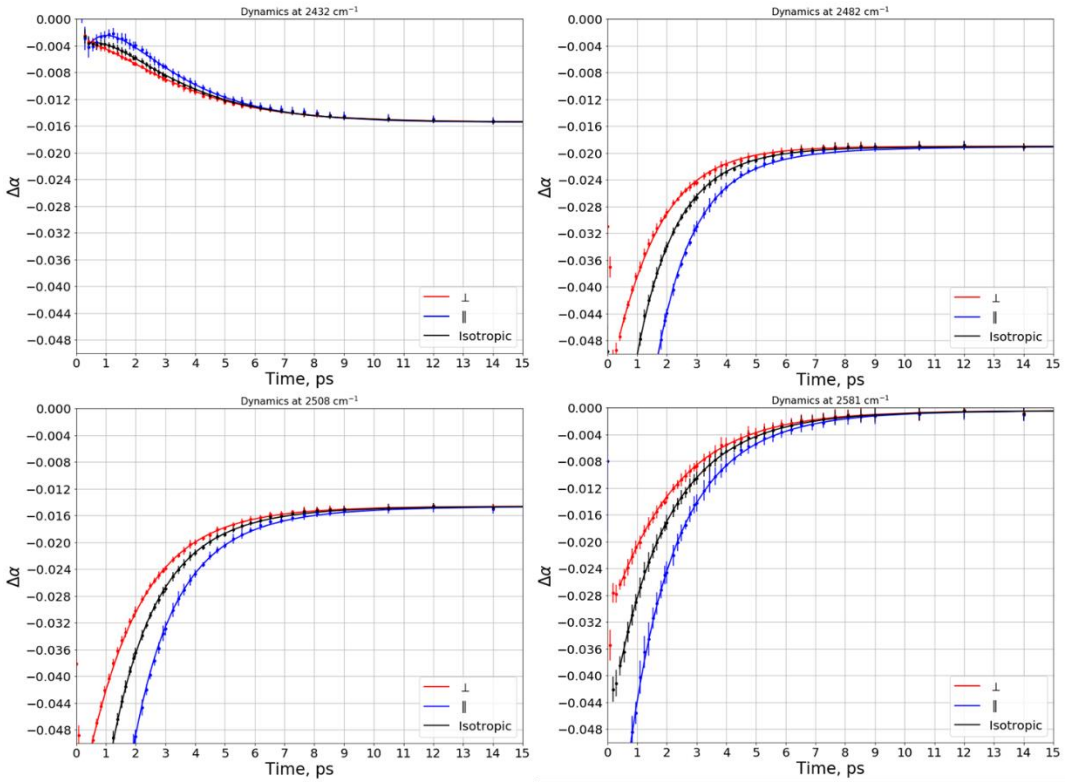

Figure S4. Dynamics at different frequencies measured for an X = 0.02 mixture. The parameter *a* was constrained to be zero, meaning that the transient absorption signal of the local hot state is assumed to be isotropic.

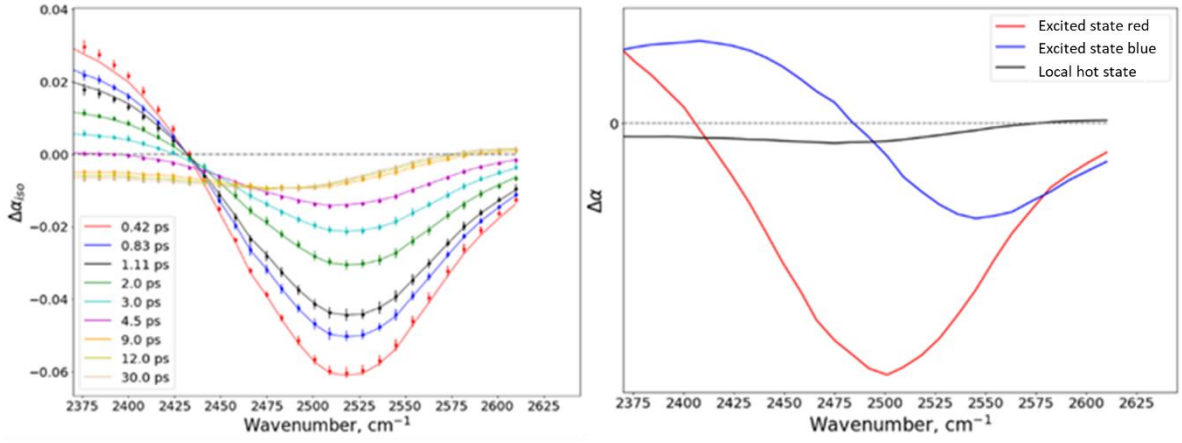

Figure S5. Transient spectra and spectral components of an X = 0.25 mixture.

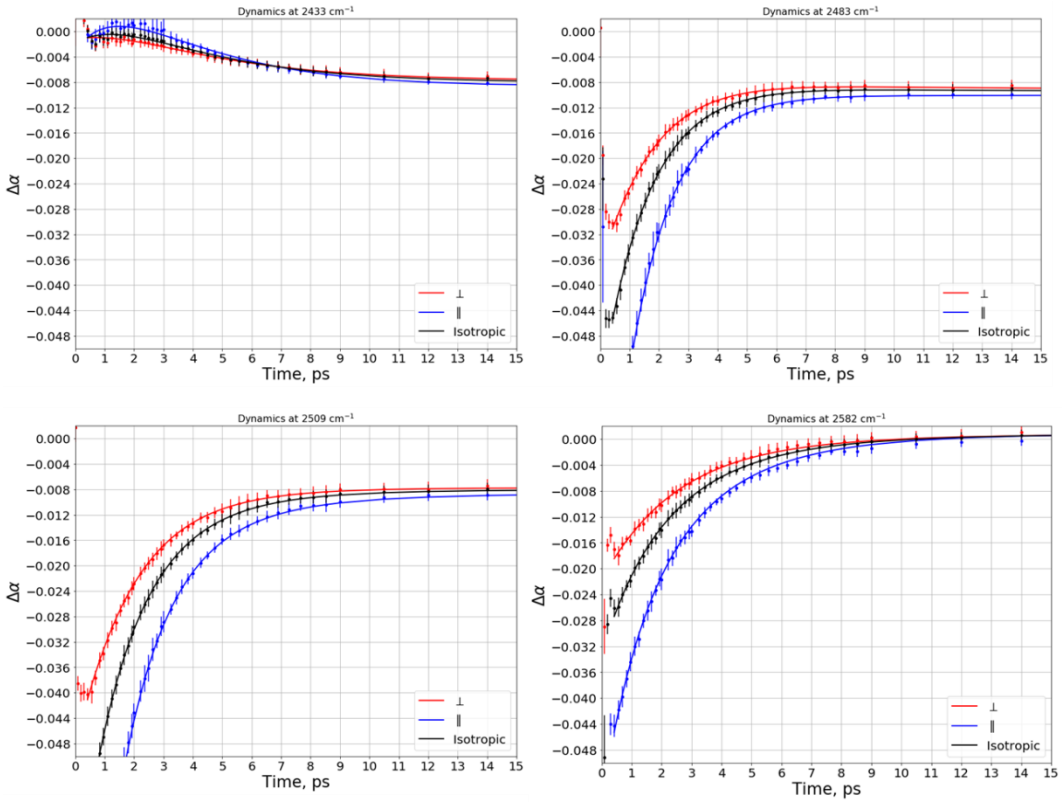

Figure S6. Dynamics at different frequencies of an X = 0.25 mixture.

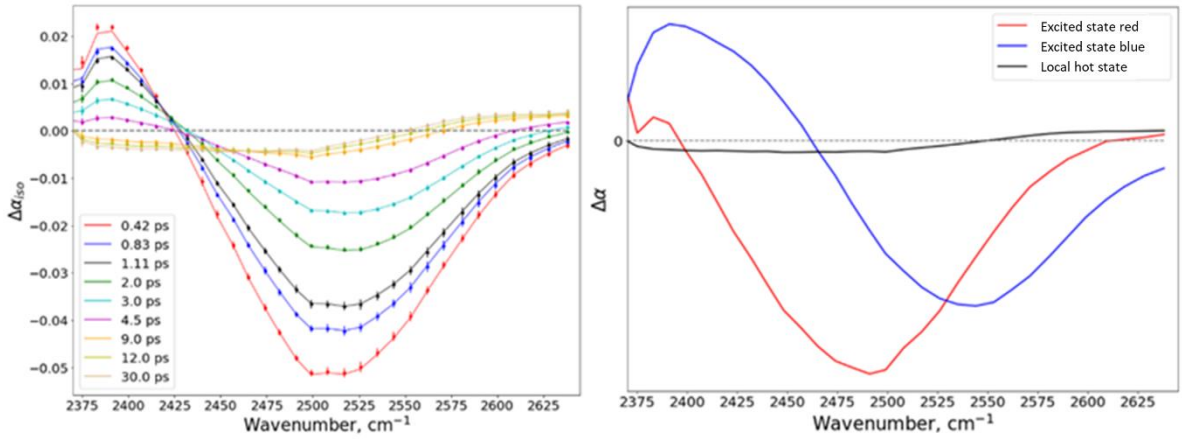

Figure S7. Transient spectra and spectral components of an X = 0.4 mixture.

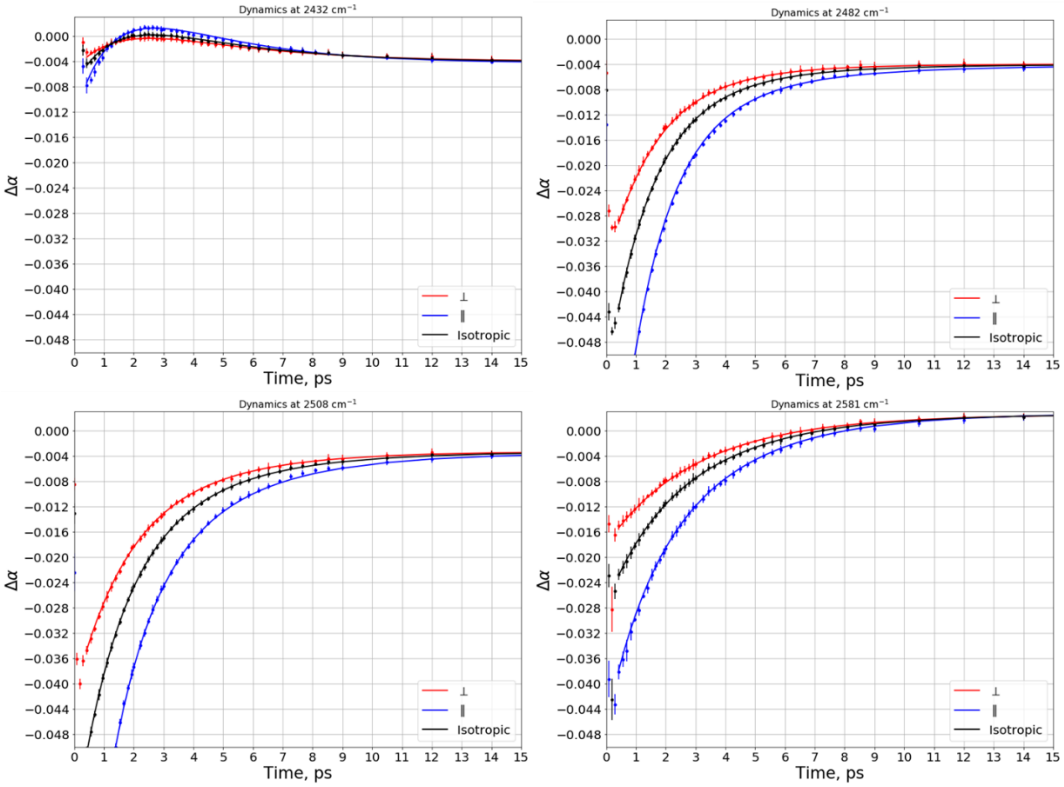

Figure S8. Dynamics at different frequencies of an X = 0.4 mixture.

Temperature dependence of the vibrational relaxation rate

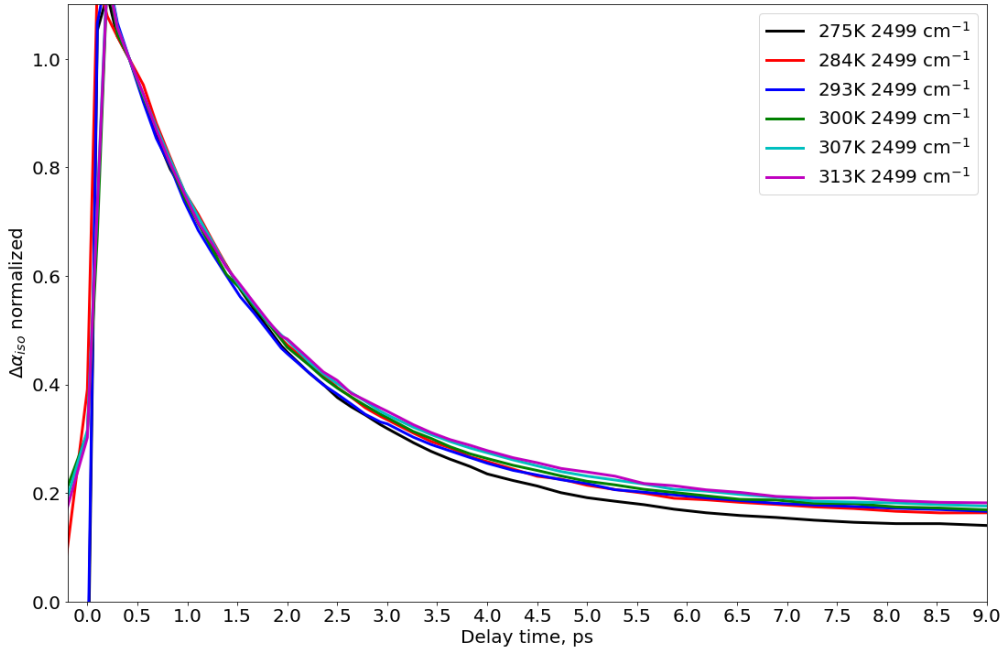

Figure S9. Dynamics of $\Delta\alpha_{iso}$ at the center of the bleaching signal of an X = 0.2 mixture at different temperatures.

Temperature dependence of the fraction and reorientation dynamics of the slow water fraction

For the water/tetramethylurea system the slow water anisotropy dynamics was shown to be strongly temperature-dependent.[3] These data could be well described assuming that the fraction of immobilized water is not changing. For the present water/2,6-lutidine system we model the

temperature dependence of the slow water fraction by varying the fractions of bulk-like and slow water molecules, keeping the time constant the same (infinitely long). The reason why these systems call for different approaches is related to the mechanism of the immobilization. In the water/TMU system water molecules are immobilized almost purely due to hydrophobic hydration while in the water/2,6-lutidine system a more complex mechanism involving both hydrophobic and hydrophilic parts of the solute applies. Additionally, for the water/2,6-lutidine system a change in temperature leads to a change of the degree of aggregation of the lutidine molecules which was not observed for the water/tetramethylurea system. Moreover, in the present study, the available temperature range was limited by the transition temperature which does not allow to explore much higher temperatures at which the reorientation time constant of the slow water molecules becomes of the order of the vibrational lifetime, which was the case for the water/tetramethylurea system.

Raw anisotropy dynamics

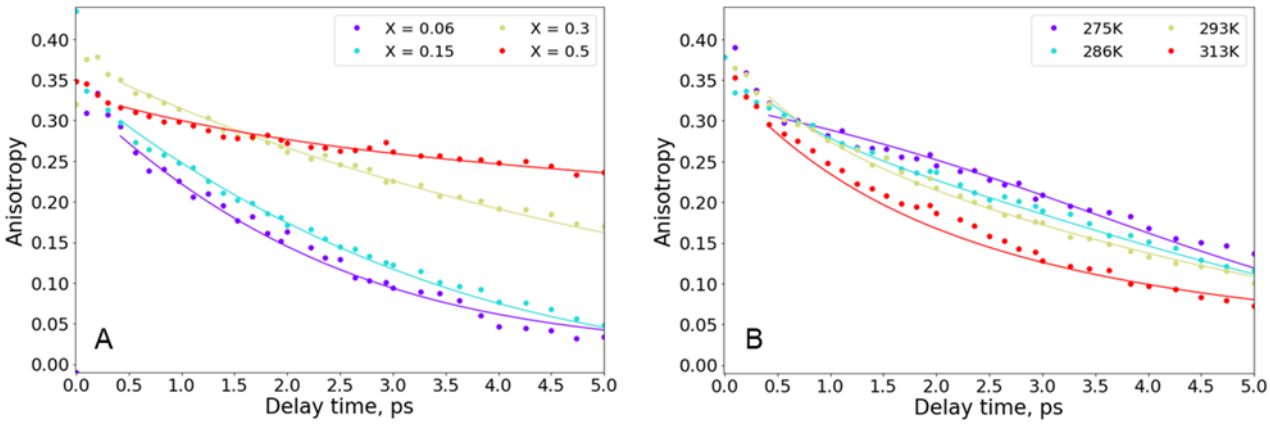

Figure S10. (A) Raw anisotropy dynamics measured at 295K (B) Raw anisotropy dynamics measured for X = 0.2. The lines represent fits based on the fits of $\Delta\alpha_{\parallel}$ and $\Delta\alpha_{\perp}$

REFERENCES

(1) Lotze, S.; Groot, C. C. M.; Vennehaug, C.; Bakker, H. J. Femtosecond Mid-Infrared Study of the Dynamics of Water Molecules in Water − Acetone and Water − Dimethyl Sulfoxide Mixtures. *J. Phys. Chem. A* **2015**, *119*, 5228–5239. https://doi.org/10.1021/jp512703w.

(2) Rezus, Y. L. A.; Bakker, H. J. Orientational Dynamics of Isotopically Diluted H2O and D2O. *J. Chem. Phys.* **2006**, *125* (144512), 1–10. https://doi.org/10.1063/1.2353831.

(3) Petersen, C.; Tielrooij, K.; Bakker, H. J. Strong Temperature Dependence of Water Reorientation in Hydrophobic Hydration Shells. *J. Chem. Phys.* **2009**, *130* (214511), 1–6. https://doi.org/10.1063/1.3142861.